RESEARCH ACTIVITIES V
Department of Applied Molecular Science

V-A Synthesis of Chiral Molecule-Based Magnets

Construction of molecule-based multifunctional materials is now becoming a challenging target. Especially, magnetic materials which have additional optical and electronic properties in the same crystals are increasing interests. Specific goals aimed for these molecule-based magnets include: i) the ability to design the molecular building blocks and to organize them in the solid for desired dimensionality, ii) the optical transparency. The physical characteristic of current interest involves optical properties, particularly with respect to natural optical activity. When a magnet has optical transparency and chiral structure, the magnetic structure of crystal expects to be a chiral spin structure. These magnets will show an asymmetric magnetic anisotropy and magneto-chiral dichroism. This category of materials don't only have scientific interest but also have the possibility for use in new devices. When we construct chiral molecule-based magnets, chirality must be controlled not only in the molecular structure, but in the entire crystal structure. As a consequence of this difficulty, only few examples of this type of magnet exist. Up to the present reported chiral magnets have low dimensional magnetic structures, the magnetic ordering temperatures are below 10 K. To afford a high-T_C magnet, dimensionality of magnetic structure must be extended in two or three dimension. When we introduce magnetic bricks, which have more than three connections for the construction of magnets, we can expect to make two or three-dimensional magnets. To make high dimensionality molecule-based magnets, we recently discovered using cyano bridged complex with chiral organic ligands.

V-A-1 Synthesis of a Novel Three-Dimensional Chiral Molecule-Based Ferrimagnet with Triple-Helical Strand Structure

IMAI, Hiroyuki; INOUE, Katsuya; KIKUCHI, Koichi[1]; YOSHIDA, Yusuke[1]; ITO, Mitsuhiro[2]; SUNAHARA, Tetsuya[2]; ONAKA, Satoru[2]
([1]IMS and Tokyo Metropolitan Univ.; [2]Nagoya Inst. Tech.)

[*Angew. Chem., Int. Ed.* **43**, 5618 (2004)]

Dark orange, hexagonal prism crystals of $[Cr(CN)_6][Mn$ D- or L-$NH_2ala]_3\cdot(3H_2O)$ were obtained by slow diffusion of $MnCl_2\cdot 4H_2O$ (1.7 mmol), D- or L-aminoalanine hydrochloride (D- or L-NH_2alaH·HCl, 2.6 mmol), and KOH (5.2 mmol) in H_2O into $K_3[Cr(CN)_6]$ (1.5 mmol) in H_2O/*iso*-propanol (1:1) mixture under argon atmosphere after several weeks. X-ray crystal structure analyses of D- and L-isomers at 100 K reveal that compounds (**1**) crystallize in the chiral space group, hexagonal $P6_3$, and consist of left- and right-handed helical structures of Mn^{II} ions, respectively (Figure 1). Each aminoalanine ion employs two types of functional groups to bridge between two adjacent Mn^{II} ions (Mn–Mn separation is 5.923 Å.). Two amino moieties and one carboxyl group within the aminoalanine ion are coordinated to two Mn^{II} ions in monodentate and bidentate coordination mode, respectively. This unique coordination leads to the construction of two differing chelating rings around the Mn^{II} ion: five- and six-membered rings. These rings align alternately resulting in the generation of extended helical chains along the *c*-axis. As expected, self-assemblies are formed between helical chains to aggregate three helical chains (Figure 2), in which the shortest Mn–Mn separation between chains is 6.517 Å. The channel structure is generated and disordered water molecules exist in the center of the triple helical strand structure (on the screw axis).

On the other hand, each $[Cr(CN)_6]^{3-}$ ion utilizes all cyanide moieties to connect between adjacent strands *via* cyanide bridges to Mn^{II} ions; as a result, a three-dimensional cyanide network is formed. The shortest and longest adjacent Cr–Mn distances through cyanide bridges are 5.490 and 5.508 Å, respectively, which are slightly longer than those in the previous crystals. The cyanide bridged network also displays basic units comprised of a helical strand structure. Each cyanide-bridged helical strand, which is composed of four metal centers (two Mn^{II} and two Cr^{III} ions) and four cyanide groups as a repeating unit characterized by a reverse turn within the helical strand of Mn^{II} and NH_2ala ions along the *c*-axis, shares the apex of the helical strand (Cr^{III} ion) between three adjacent helical strands (Figure 1).

This compound exhibits ferrimagnetic behavior essentially below 35 K. The magnetic transition temperature of this compound is relatively low despite formation of a three-dimensional cyanide network. This phenomenon is probably attributable to the comparatively long cyanide-bridged distance in this crystal. In addition, it may result consequent to the occurrence of spin frustration between manganese ions within the triple helical strand at high temperature. Below 35 K, the spin on manganese alone survives due to the ferrimagnetic coupling between manganese and chromium ions. From a physical standpoint, this phenomenon is the focus of interesting research, as the spin structure of this compound is also expected to possess triple helical nature. Some chiral molecule-based magnets have been prepared previously; however, at present, a chiral helical spin structure has not been documented. It is one of the reasons affording an explanation as to why a crystal forming a helical structure has never been synthesized. Thus, it is certain that this molecule is a suitable candidate for this endeavor. Magnetization measurements, μSR (muon spin resonance) spectroscopy and neutron diffraction of a single crystal will lead

to characterization of the details of magnetic structure in this compound.

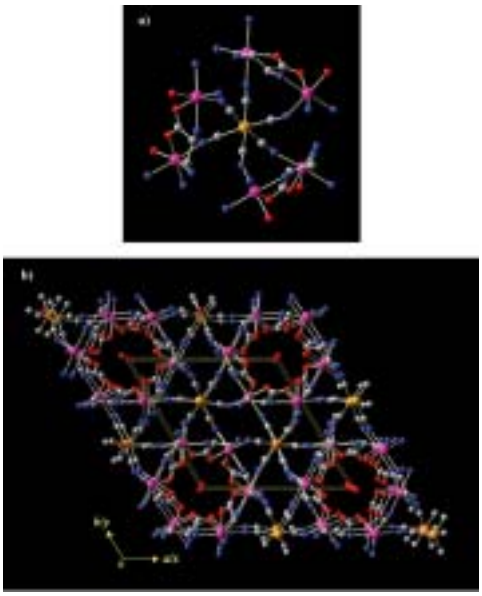

Figure 1. a) Coordination geometry of the heptanuclear unit of $[Cr^{III}(CN)_6][Mn^{II}$ L-$NH_2ala]_3 \cdot (3H_2O)$ (**1**). b) Overall view of crystal structure of $[Cr^{III}(CN)_6][Mn^{II}$ L-$NH_2ala]_3 \cdot (3H_2O)$ (**1**) along the *c*-axis. Cr atoms are shown in yellow brown, Mn in purple, C in gray N in blue and O in red. The hydrogen atoms are omitted for simplicity.

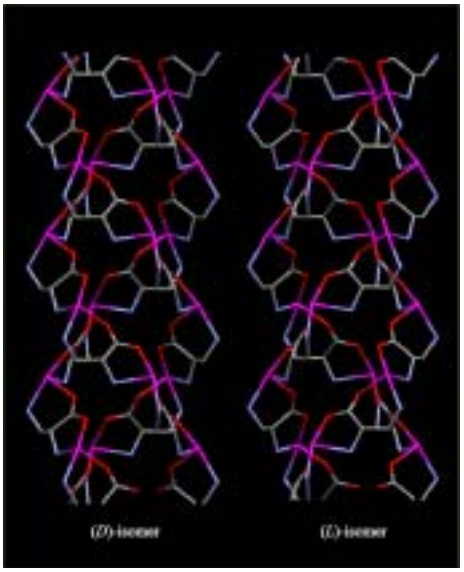

Figure 2. Capped sticks models of a left-handed and a right-handed triple strands in $[Cr^{III}(CN)_6][Mn^{II}$ D or L-$NH_2ala]_3 \cdot (3H_2O)$ (**1**). Mn atoms are shown in purple, C in gray N in blue and O in red.

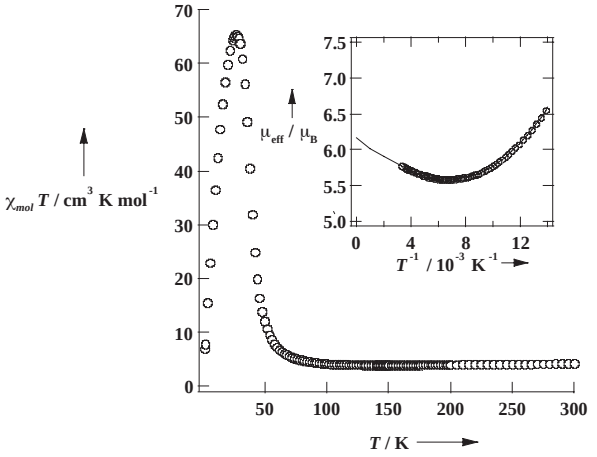

Figure 3. $\chi_{mol}T$ *versus* T plot at 5000 G of $[Cr^{III}(CN)_6][Mn^{II}$ D or L-$NH_2ala]_3 \cdot (3H_2O)$ (**1**). Inset: Plot of effective magnetic moment *versus* 1/*T*.

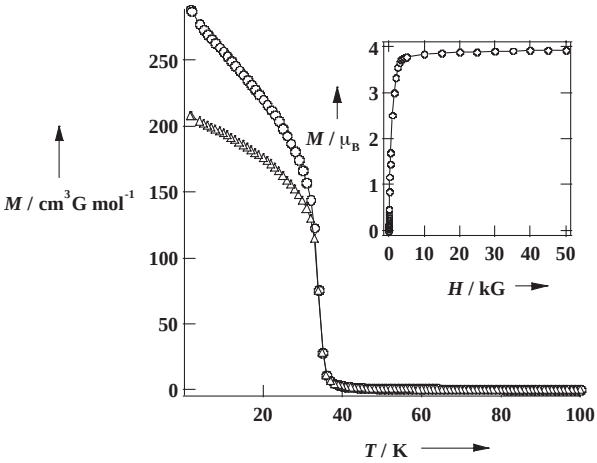

Figure 4. Temperature dependence of magnetization of $[Cr^{III}(CN)_6][Mn^{II}$ D- or L-$NH_2ala]_3 \cdot (3H_2O)$ (**1**). The FC (triangle) and ZFC (circle) magnetizations at 5 G are shown. Inset: Field dependence of magnetization of $[Cr^{III}(CN)_6][Mn^{II}$ D- or L-$NH_2ala]_3 \cdot (3H_2O)$ (**1**) at 2 K.

V-A-2 TOF Neutron Powder Diffraction Studies on a Chiral Two-Dimensional Molecule-Based Magnet

HOSHIKAWA, Akinori[1]; KAMIYAMA, Takashi[1]; PURWANTO, Agus[1,2]; OHISHI, Kazuki[1]; HIGEMOTO, Wataru[1]; ISHIGAKI, Toru[3]; IMAI, Hiroyuki; INOUE, Katsuya
([1]KEK; [2]Natl. Nuclear Energy Agency, Indonesia; [3]Muroran Inst. Tech.)

[*J. Phys. Soc. Jpn.* **73**, 2597 (2004)]

The magnetic structure of a chiral molecule-based magnet, $[Cr(CN)_6][Mn(S)$-pnH$(H_2O)](H_2O)$ (Space group = $P2_12_12_1$, Figure 1), has been studied by neutron powder diffraction as a function of temperature from 4 K to 300 K. The 020 and 022 magnetic reflections were clearly observed below T_C = 38 K (Figure 2). From the intensity analysis of magnetic reflections, it was concluded that the magnetic structure is non-collinear ferrimagnetic with the magnetic (Shubnikov) space

group $P2_12_1'2_1'$, and magnetic moments of Cr and Mn atoms are mutually antiparallel along a direction near the *a*-axis. Our result implies that the long-period magnetic structure, if exists, is not a helical structure but a conical one.

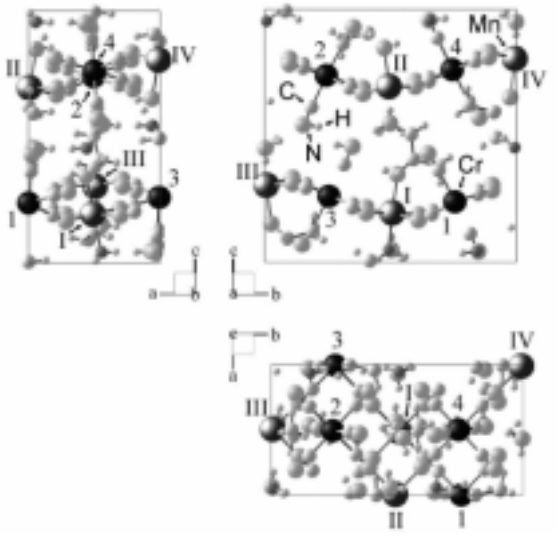

Figure 1. Crystal structure of $[Cr(CN)_6][Mn(S)\text{-}pnH(H_2O)](H_2O)$. Magnetic atoms Cr and Mn are marked with the Arabic and Roman numerals, respectively.

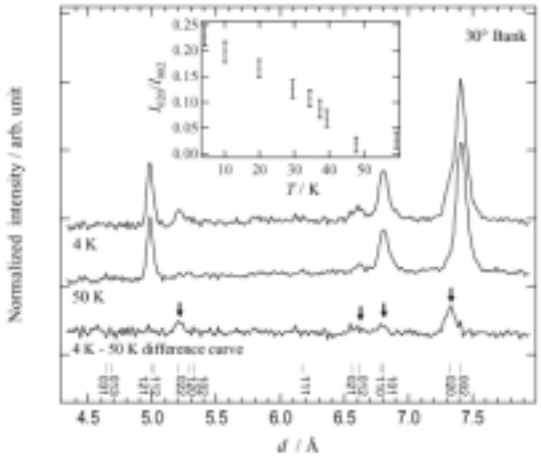

Figure 2. The neutron diffraction patterns at 4 K (below T_C) and 50 K (above T_C), and their difference pattern of $[Cr(CN)_6][Mn(S)\text{-}pnH(H_2O)](H_2O)$ obtained by the 30 degree bank of the Vega diffractometer. The difference pattern shows the magnetic contribution only. Intensities are normalized by the incident spectrum. The inset shows the temperature dependence of the intensity ratio of the 020 magnetic Bragg reflection to the 002 nuclear Bragg one, I020/I002.

V-B Nano-Structure in Metal Oxides Prepared by Synchrotron Radiation and Swift Heavy Ions

In the project, micro-nano fabrication technique for metal oxide has been examined. The first one is the deep x-ray lithography and the liquid phase deposition method. Periodic arrangements of titanium dioxide (TiO_2) micro structure projections were fabricated in a supersaturated aqueous solution using ordered microcavities of poly (methylmethacrylate) as a template. The shape and periodicity of the TiO_2 projections were strictly controlled with the depth and arrangement of the cavities because crystalline TiO_2 was uniformly grown on the organic surface through heterogeneous nucleation. This biomimetic route is applicable to designed synthesis of three-dimensional architectures for photonic structures of various metal oxides. The other method is by using of the latent tracks introduced by the swift heavy ion. Micro structure having nano-order flatness was achieved after chemical etching. This method can be applied to create photonic crystal structure of titanium dioxide.

V-B-1 Photoinduced Hydroxylation at ZnO Surface

ASAKUMA, Naoko[1]; FUKUI, Toshimi[2]; TOKI, Motoyuki[2]; AWAZU, Koichi[3]; IMAI, Hiroaki[1]
([1]Keio Univ.; [2]KRI.; [3]IMS and AIST)

[*Thin Solid Films* **445**, 284–287 (2003)]

We observed UV-stimulated hydroxylation at the surface of ZnO crystals. Reactive defective sites were initially formed in the surface layer via photoreduction induced with energetic photons above the band gap of ZnO. Hydroxyl groups were produced by a chemical reaction of the photoinduced defective sites with water molecules in the atmosphere. Two types of hydroxyl groups were found at the irradiated surface because two kinds of defective sites were induced with the UV illumination.

V-B-2 Ablation and Compaction of Amorphous SiO_2 Irradiated with ArF Excimer Laser

AWAZU, Koichi[1]
([1]IMS and AIST)

[*J. Non-Cryst. Solids* **337**, 241–253 (2004)]

The structure of amorphous SiO_2 exposed to ArF excimer laser irradiation was examined. Threshold fluence for causing ablation with a single pulse depended on sample preparation: more specifically, 1 J/cm^2 for thermally grown SiO_2 films on silicon and 2.5 J/cm^2 for bulk SiO_2. It was found that the bond angle of Si–O–Si was reduced by irradiation near the interface of thermally grown SiO_2 films. In contrast, evolution of the bond angle by irradiation was absent in both the bulk SiO_2 and SiO_2 film-near the top surface, even though the concentration of puckered four-menmered rings deduced from Raman spectra dramatically increased. It is assumed that planar three-membered rings were generated in the SiO_2 thin layer near the interface, and puckered four-membered rings were generated in the bulk SiO_2. The concentration of both the Si^{3+} and Si^{2+} structure was increased at a fluence of 800 mJ/cm^2 with an increasing number of pulses, although generation of both was absent at higher fluence for a single pulse. The author proposes that the structure of SiO_2 is created by flash heating and quenching by pulse laser irradiation. Structural similarities were found between the irradiated SiO_2 and SiO_2 at high temperatures.

V-C Bioinorganic Chemistry and Structural Biology of Heme Proteins

One of research activities of my group is directed toward developing a rigorous, quantitative understanding of the biochemical function of heme proteins such as oxygenases, peroxidases and oxidases by characterization of their structural and functional properties. We use different experimental strategies including protein engineering, spectroscopic characterization of the molecular structure of the active centers, measurements of dynamics of substrates and inhibitor binding, and X-ray crystallography.

My current heme protein projects include (1) elucidation of the catalytic mechanism of heme oxygenase, one of the essential components of the heme catabolism and biosynthesis of carbon monoxide, a versatile physiological messenger molecule, (2) elucidation of the mechanism of controlling reactivity of hemoglobin and myoglobin, and (3) determination of heme sensing mechanism of Bach1, a heme-dependent transcription factor which regulates heme oxygenase gene expression. Effective clues to delineate the detailed active site structure have been obtained by X-ray crystallography, resonance Raman and magnetic resonance studies. The synergy of site-directed mutagenesis, structural biology, and spectroscopic techniques has revealed the specific roles of amino acids located in the active centers of heme proteins. Ligands and substrates binding measurements complement the structural data for our understanding functional properties displayed by heme proteins at the molecular level.

V-C-1 Kinetic Isotope Effects on the Rate-Limiting Step of Heme Oxygenase Catalysis Indicate Concerted Proton Transfer/Heme Hydroxylation

DAVYDOV, Roman[1]; MATSUI, Toshitaka[2]; FUJII, Hiroshi; IKEDA-SAITO, Masao[3]; HOFFMAN, Brian M.[1]
([1]Northwestern Univ.; [2]Tohoku Univ.; [3]IMS and Tohoku Univ.)

[*J. Am. Chem. Soc.* **125**, 16208–16209 (2003)]

Heme oxygenase (HO) catalyzes the O_2 and NADPH/cytochrome P450 reductase-dependent conversion of heme to biliverdin, free iron ion, and CO through a process in which the heme participates both as dioxygen-activating prosthetic group and substrate. We earlier confirmed that the first step of HO catalysis is a monooxygenation in which the addition of one electron and two protons to the HO oxy-ferroheme produces ferric-α-*meso*-hydroxyheme (**h**). Cryoreduction/EPR and ENDOR measurements further showed that hydroperoxo-ferri-HO converts directly to **h**, in a single kinetic step without formation of a Compound I. We here report details of that rate-limiting step. One-electron 77 K cryoreduction of human oxy-HO and annealing at 200 K generates a structurally relaxed hydroperoxo-ferri-HO species, denoted **R**. We here report the cryoreduction/annealing experiments that *directly* measure solvent and secondary kinetic isotope effects (KIEs) of the rate-limiting **R** to **h** conversion, using enzyme prepared in H_2O/D_2O buffers to measure the solvent KIE (*solv*-KIE), and the secondary KIE (*sec*-KIE) associated with deuteration of the heme *meso*-carbons. This approach is unique in that KIEs measured by monitoring the rate-limiting step are not susceptible to masking by KIE's of other processes, and these results represent the first direct measurement of the KIE's of product formation by a kinetically competent reaction intermediate in *any* dioxygen-activating heme enzyme. The observation of *both solv*-KIE(298) = 1.8 and *sec*-KIE(298) = 0.8 (inverse) indicates that the rate-limiting step for formation of **h** by HO is a concerted process: proton transfer to the hydroperoxo-ferri-heme through the distal-pocket H-bond network, likely from a carboxyl group acting as a general acid catalyst, occurring in synchrony with attack of 'OH^+' on the α-*meso* carbon to form a tetrahedral hydroxylated-heme intermediate. Subsequent rearrangement and loss of H_2O then generates **h**.

V-C-2 FeNO Structure in Distal Pocket Mutants of Myoglobin Based on Resonance Raman Spectroscopy

COYLE, Candace M.[1]; VOGEL, Kathleen M.[1]; RUSH, Thomas S. III[1]; KOZLOWSKI, Pawel M.[1]; WILLIAMS, Robert[1]; SPIRO, Thomas, G.[1]; DOU, Yi[2]; IKEDA-SAITO, Masao[3]; OLSON, John S.[4]; ZGIERSKI, Marek Z.[5]
([1]Princenton Univ.; [2]Case Western Reserve Univ.; [3]IMS and Tohoku Univ.; [4]Rice Univ.; [5]Natl. Res. Council Canada)

[*Biochemistry* **42**, 4896–4903 (2003)]

FeNO vibrational frequencies were investigated for a series of myoglobin mutants using isotopeedited resonance Raman spectra of $^{15/14}$NO adducts, which reveal the FeNO and NO stretching modes. The latter give rise to doublet bands, as a result of Fermi resonances with coincident porphyrin vibrations; these doublets were analyzed by curve-fitting to obtain the νNO frequencies. Variations in νNO among the mutants correlate with the reported νCO variations for the CO adducts of the same mutants. The correlation has a slope near unity, indicating equal sensitivity of the NO and CO bonds to polar influences in the heme pocket. A few mutants deviate from the correlation, indicating that distal interactions differ for the NO and CO adducts, probably because of the differing distal residue geometries. In contrast to the strong and consistent νFeC/νCO correlation found for the CO adducts, νFeN correlates only weakly with νNO, and the slope of the correlation depends on which residue is being mutated.

This variability is suggested to arise from steric interactions, which change the FeNO angle and therefore alter the Fe–NO and N–O bond orders. This effect is modeled with Density Functional Theory (DFT) and is rationalized on the basis of a valence isomer bonding model. The FeNO unit, which is naturally bent, is a more sensitive reporter of steric interactions than the FeCO unit, which is naturally linear. An important additional factor is the strength of the bond to the proximal ligand, which modulates the valence isomer equilibrium. The FeNO unit is bent more strongly in MbNO than in protein-free heme-NO complexes because of a combination of a strengthened proximal bond and distal interactions.

V-C-3 The Crystal Structures of the Ferric and Ferrous Forms of the Heme Complex of HmuO, a Heme Oxygenase of *Corynebacterium diphtheriae*

HIROTSU, Shoko[1]; CHU, Grace C.[2]; UNNO, Masaki[1]; LEE, Dong-Sun[3]; YOSHIDA, Tadashi[4]; PARK, Sam-Yong[3]; SHIRO, Yoshitsugu[3]; IKEDA-SAITO, Masao[5]
([1]Tohoku Univ.; [2]Case Western Reserve Univ.; [3]RIKEN Harima Inst./SPring-8; [4]Yamagata Univ.; [5]IMS and Tohoku Univ.)

[*J. Biol. Chem.* **279**, 1197–11947 (2004)]

Crystal structures of the ferric and ferrous heme complexes of HmuO, a 24 kDa heme oxygenase of *Corynebacterium diphtheriae*, have been refined to 1.4 and 1.5 Å resolution, respectively. The HmuO structures show that the heme group is closely sandwiched between the proximal and distal helices. The imidazole group of His20 is the proximal heme ligand, which closely eclipses the β and δ meso axis of the porphyrin ring. A long range hydrogen bonding network is present, connecting the iron-bound water ligand to the solvent water molecule. This enables proton transfer from the solvent to the catalytic site, where the oxygen activation occurs. In comparison to the ferric complex, the proximal and distal helixes move closer to the heme plane in the ferrous complex. Together with the kinked distal helix, this movement leaves only the α-meso carbon atom accessible to the iron-bound dioxygen. The heme pocket architecture is responsible for stabilization of the ferric hydroperoxo active intermediate by preventing premature heterolytic O–O bond cleavage. This allows the enzyme to oxygenate selectively at the α-meso carbon in HmuO catalysis.

V-C-4 Crystal Structure of the Dioxygen-Bound Heme Oxygenase from *Corynebacterium diphtheriae*: Implications for Heme Oxygenase Function

UNNO, Masaki[1]; MATSUI, Toshitaka[1]; CHU, Grace C.[2]; COUTURE, Manon[3]; YOSHIDA, Tadashi[4]; ROUSSEAU, Denis L.[3]; OLSON, John S.[5]; IKEDA-SAITO, Masao[6]
([1]Tohoku Univ.; [2]Case Western Reserve Univ.; [3]Albert Einstein College Med.; [4]Yamagata Univ.; [5]Rice Univ.; [6]IMS and Tohoku Univ.)

[*J. Biol. Chem.* **279**, 21055–21061 (2004)]

HmuO, a heme oxygenase of *Corynebacterium diphtheriae*, catalyzes degradation of heme using the same mechanism as the mammalian enzyme. The oxy form of HmuO, the precursor of the catalytically active ferric hydroperoxo species, has been characterized by ligand binding kinetics, resonance Raman spectroscopy, and X-ray crystallography. The oxygen association and dissociation rate constants are 5 μM^{-1} s^{-1} and 0.22 s^{-1}, respectively, yielding an O_2 affinity of 21 μM^{-1} that is ~20 times greater than that of mammalian myoglobins. However, the affinity of HmuO for CO is only 3 to 4-fold greater than that for mammalian myoglobins, implying the presence of strong hydrogen bonding interactions in the distal pocket of HmuO that preferentially favor O_2 binding. Resonance Raman spectra show that the Fe–O_2 vibrations are tightly coupled to porphyrin vibrations, indicating a highly bent Fe–O–O geometry that is characteristic of the oxy forms of heme oxygenases. In the crystal structure of the oxy form, the Fe–O–O angle is 110°; the O–O bond is pointed toward the heme α-*meso*-carbon by direct steric interactions with Gly135 and Gly139; and hydrogen bonds occur between the bound O_2 and the amide nitrogen of Gly139 and a distal pocket water molecule, which is a part of an extended hydrogen bonding network that provides the solvent protons required for oxygen activation. In addition the O–O bond is orthogonal to the plane of the proximal imidazole side chain, which facilitates hydroxylation of the porphyrin α-*meso*-carbon by preventing premature O–O bond cleavage.

V-C-5 Heme Regulates Gene Expression by Triggering Crm1-Dependent Nuclear Export of Bach1

SUZUKI, Hiroshi[1]; TASHIRO, Satoshi[1]; HIRA, Shusuke[2]; SUN, Jiying[1]; YAMAZAKI, Chikara[1]; ZENKE, Yukari[1]; IKEDA-SAITO, Masao[3]; YOSHIDA, Minoru[4]; IGARASHI, Kazuhiko[1]
([1]Hiroshima Univ.; [2]Tohoku Univ.; [3]IMS and Tohoku Univ.; [4]RIKEN)

[*EMBO J.* **23**, 2544–2553 (2004)]

Bach1 is a transcriptional repressor of heme oxygenase-1 and β-globin genes, both of which are known to be transcriptionally induced by heme. To test the hypothesis that heme regulates the activity of Bach1, we expressed wild-type and mutated versions of Bach1 together with or without its heterodimer partner MafK in human 293T and GM02063 cells and examined their subcellular localization. Inhibition of heme synthesis enhanced the nuclear accumulation of Bach1 whereas treating cells with hemin resulted in nuclear exclusion of Bach1. While the cadmium-inducible nuclear export signal of Bach1 was dispensable for the heme response, a region containing two of the heme-binding motifs were found to be critical for the heme-induced nuclear exclusion. This region functioned as a heme-regulated nuclear export signal dependent on the exporter Crm1. These results extend the regulatory roles for heme in protein sorting, and suggest that Bach1 transduces metabolic activity into gene expression.

V-D Pro-Oxidants-Induced Iron Release from the Fe-S Cluster of Mitochondrial Aconitase and Its Prevention by Flataxin

Pro-oxidants, such as hydrogen peroxide and superoxide anion, are highly toxic for many living organisms. One of the adverse effects of pro-oxidants is modulation of mitochondrial respiration. Using EPR spectroscopy, we have identified that pro-oxidants deactivates mitochondrial aconitase, the key enzyme in citrate cycle, by releasing one of Fe from the 4Fe-4S cluster, and that mitochondria is surprisingly equipped a recovery mechanism to restore the active 4Fe-4S cluster. We have recently discovered that this restoration is achieved by an iron insertion from frataxin, an iron storage protein in mitochondria, which functions as an iron chaperon protein. We are in the process of elucidation of the inter protein iron transfer mechanism from frataxin to aconitase at molecular level.

V-D-1 Redox-Dependent Modulation of Aconitase Activity in Intact Mitochondria

BULTEAU, Anne-Laure[1]; IKEDA-SAITO, Masao[2]; SZWEDA, Luke I.[1]
([1]Case Western Reserve Univ.; [2]IMS and Tohoku Univ.)

[*Biochemistry* **42**, 14846–14855 (2003)]

It has previously been reported that exposure of purified mitochondrial or cytoplasmic aconitase to superoxide ($O_2^{\bullet-}$) or hydrogen peroxide (H_2O_2) leads to release of the Fe-α from the enzyme's $[4Fe–4S]^{2+}$ cluster and to inactivation. Nevertheless, little is known regarding the response of aconitase to pro-oxidants within intact mitochondria. In the present study, we provide evidence that aconitase is rapidly inactivated and subsequently reactivated when isolated cardiac mitochondria are treated with H_2O_2. Reactivation of the enzyme is dependent on the presence of the enzyme's substrate, citrate. EPR spectroscopic analysis indicates that enzyme inactivation precedes release of the labile Fe-a from the enzyme's $[4Fe–4S]^{2+}$ cluster. In addition, as judged by isoelectric focusing gel electrophoresis, the relative level of Fe-α release and cluster disassembly does not reflect the magnitude of enzyme inactivation. These observations suggest that some form of posttranslational modification of aconitase other than release of iron is responsible for enzyme inactivation. In support of this conclusion, H_2O_2 does not exert its inhibitory effects by acting directly on the enzyme, rather inactivation appears to result from interaction (s) between aconitase and a mitochondrial membrane component responsive to H_2O_2. Nevertheless, prolonged exposure of mitochondria to steady-state levels of H_2O_2 or ($O_2^{\bullet-}$) results in disassembly of the $[4Fe–4S]^{2+}$ cluster, carbonylation, and protein degradation. Thus, depending on the pro-oxidant species, the level and duration of the oxidative stress, and the metabolic state of the mitochondria, aconitase may undergo reversible modulation in activity or progress to $[4Fe–4S]^{2+}$ cluster disassembly and proteolytic degradation.

V-D-2 Frataxin Acts as an Iron Chaperone Protein To Modulate Mitochondrial Aconitase Activity

BULTEAU, Anne-Laure[1]; O'NEILL, Heather A.[2]; KENNEDY, Mary Claire[3]; IKEDA-SAITO, Masao[4]; ISAYA, Grazia[2]; SZWEDA, Luke I.[1]
([1]Case Western Reserve Univ.; [2]Mayo Clinic College Med.; [3]Gannon Univ.; [4]IMS and Tohoku Univ.)

[*Science* **305**, 242–245 (2004)]

Friedreich's ataxia is a genetic disorder characterized by a deficiency in frataxin, the mitochondrial iron-binding protein. We have identified a role for frataxin as an iron chaperone protein that is required for the reversible modulation of mitochondrial aconitase activity in response to pro-oxidants. By protecting Fe-S clusters from disassembly, frataxin can prevent iron accumulation and production of the highly reactive and toxic hydroxyl radical. Alterations in the level, structure, and chaperone function of frataxin may participate in the progression of degenerative disorders associated with declines in aconitase and mitochondrial activity.

V-E Quantum Emissions from Solid in Femtosecond Intense Laser Field

Quantum emissions, which are high-energy electron, ion and photon beams, generated by interaction of ultrashort intense laser field with matter has recently been attracting considerable attention because of interest in fundamental photosciences and its potential applications in compact accelerator, proton therapy and materials sciences. We have studied a mechanism of quantum emissions (especially on hard X-ray and fast protons) form metal target in intense laser field.

V-E-1 Hard X-Ray Emission from a Cooper Target by Focusing a Picosecond Laser Beam at 3 x 10^{13} W/cm^2

NAGAO, Hirofumi[1]; HIRONAKA, Yoichiro[1]; NAKAMURA, Kazutaka[2]; KONDO, Ken-ichi[1]
([1]Tokyo Inst. Tech.; [2]IMS and Tokyo Inst. Tech.)

[*Jpn. J. Appl. Phys.* **43**, 1207–1208 (2004)]

Hard X-ray pulses are generated by focusing a picosecond laser beam (25-ps, 1064 nm) on a copper target in air at an intensity of 3×10^{13} W/cm^2. X-ray energy is measured using an X-ray charge-coupled device. The obtained spectrum consists of strong K_α and K_β emissions and a weak continuum at an energy range of 4–10 keV. The photon numbers of the hard X-rays (4–10 keV) were estimated to be approximately 4000 photons/4πsr/pulse.

V-E-2 Enhanced Generation of Fast Protons from a Polymer-Coated Metal Foil by a Femtosecond Intense Laser Field

KISHIMURA, Hiroaki[1]; MORISHITA, Hiroto[1]; OKANO, Yasuhisa[1]; OKANO, Yasuaki[1]; HIRONAKA, Yoichiro[1]; KONDO, Ken-ichi[1]; NAKAMURA, Kazutaka[2]; OISHI, Yuji[3]; NEMOTO, Koshichi[3]
([1]Tokyo Inst. Tech.; [2]IMS and Tokyo Inst. Tech.; [3]CREIPT)

[*Appl. Phys. Lett.* **85**, 2736–2738 (2004)]

The results of generation of fast protons from 5-μm thick copper foil targets by 60 fs laser irradiation at 1.5×10^{17} W/cm^2 are presented. Both poly-vinyl-methyl-ether (PVME)-coated and uncoated copper foil targets are examined. Fast protons are measured using a Thomson mass spectrometer and maximum proton energies are 570 keV and 280 keV for the PVME-coated and the uncoated target, respectively. The intensity of fast protons with energy of 160 keV from the PVME-coated target is approximately 80-fold higher than that from the uncoated target.